

High Light-to-Energy Conversion Efficiencies for Solar Cells Based on Nanostructured ZnO Electrodes

H. Rensmo, K. Keis, H. Lindström, S. Södergren, A. Solbrand, A. Hagfeldt,* and S.-E. Lindquist*

Department of Physical Chemistry, Uppsala University, Box 532, S-75121 Uppsala, Sweden

L. N. Wang and M. Muhammed

Department of Inorganic Chemistry, Royal Institute of Technology, S-100 44 Stockholm, Sweden

Received: September 23, 1996; In Final Form: January 16, 1997[®]

Photoelectrochemical properties of nanostructured ZnO thin film electrodes have been investigated in the UV and visible regions. For films consisting of 15 nm large undoped crystallites a maximum monochromatic current conversion efficiency of 58% was obtained in the visible using a ruthenium-based dye as a sensitizer. The overall solar energy conversion efficiency for this film was 2%. In comparison, sensitized films consisting of 150 nm large Al-doped crystallites yield a monochromatic current conversion efficiency of 31% and an overall solar energy conversion efficiency of 0.5%. The study also shows that nanostructured ZnO may give high efficiencies in the UV region, approaching unity for the Al-doped films.

Introduction

Dye-sensitized semiconducting single-crystal ZnO electrodes were studied early by Gerischer and Tributsch.^{1–3} Later it was shown that with an increased effective surface area of the ZnO electrode the photocurrents could be considerably improved.⁴ Today the most promising dye-sensitized system is based on a nanostructured network of TiO₂, resulting in a very high internal area.^{5–9} Photons-to-current conversion properties of a number of semiconducting nanostructured materials have been reported, e.g., TiO₂,¹⁰ SnO₂,¹¹ Fe₂O₃,¹² ZnO,¹³ CdS, and CdSe.¹⁴ Dye-sensitized nanostructured electrodes, other than TiO₂, are much less studied. For ZnO Redmond et al.¹⁵ obtained overall solar-to-energy conversion efficiencies of 0.4% for films based on 10 nm large ZnO crystallites.

That thorough investigations of different materials should be worthwhile doing is especially true for nanostructured electrodes where not only the inherent properties of the nanocrystallites such as band gap, band gap position, and surface structure are important. The whole system must be taken into account in optimizing a particular application. Particle size and shape, porosity, necking structure, film thickness, distance between electrodes, electrolyte composition, and illumination direction may all be factors of significant importance. It is also essential to compare different materials for a fundamental understanding of nanostructured systems.

Today most of the research concerning nanostructured systems is based on particles around 5–30 nm in size. In this article we report the fabrication and photoconversion properties of sensitized and unsensitized Al-doped nanostructured ZnO films based on particles around 1 order of magnitude larger (roughly 150 nm in diameter). The excellent photoconversion properties obtained with these films demonstrate the broad range of particle sizes that can be used in nanostructured systems. Encouraged by the high conversion efficiencies for nanostructured ZnO films based on large Al-doped crystallites, we also report on high efficiencies for films consisting of smaller and undoped particles. The possibility of using ZnO as the

nanocrystallite material in a highly efficient regenerative solar cell is discussed.

Experimental Section

The different ZnO powders were synthesized as follows.¹⁶ Solutions of 1 M ZnCl₂ containing 0.02 M AlCl₃ and 1 M NH₄-CO₂NH₂ were prepared by dissolution of the corresponding salt (reagent grades) in distilled water. Equal amounts of the two solutions were added to a reactor, while stirring. A white precipitate was instantly formed, and evolution of gas was observed. The precipitate was filtered off, washed with water, dried at 100 °C, and then calcined at 350 °C for 3 h to give an ultrafine yellowish-white powder of ZnO. When heated, a small amount of oxygen is lost from the lattice, resulting in a nonstoichiometric Zn_{1+x}O phase ($x < 70$ ppm) that is slightly yellow.¹⁷ This powder is referred to as ZnO (A) below. The synthesis of the second powder, referred to as ZnO (B) below, is similar except that no AlCl₃ was added during precipitation.

Dispersions of the ZnO powders were prepared in a similar way as described earlier for TiO₂ powder.⁶ A paste of 3 g of powder, 0.1 mL acetylacetone, and 1 mL of water/acetylacetone mixture (10/1) was ground in a mortar. A total amount of 1 mL of the water/acetylacetone mixture was added in 0.1 mL portions during continuous grinding, resulting in a viscous solution. Triton-X (0.1 μ L) was added while stirring the mixture carefully, using a magnetic stirrer. During the stirring, 3.2 mL water was added to the dispersion based on powder A and 0.5 mL of water to the dispersion based on powder B, respectively. All chemicals used were of reagent grade; the water used was Milli-Q (Millipore Corporation). The resulting dispersions were spread onto transparent conducting glass sheets (Libbey Owens Ford (LOF), fluorine-doped SnO₂ glass, sheet resistance 8 Ω /square). By use of Scotch tape as a spacer, thin films were formed by raking off the excess colloidal solution with a glass rod. The thinnest films were prepared by spin coating using a diluted dispersion. The samples were sintered in air at 430 °C for 30 min. Dye sensitization of the nanostructured electrodes was carried out by soaking the film in an ethanol solution of a ruthenium complex, *cis*-bis(4,4'-dicarboxy-2,2'-bipyridine)-bis-(isothiocyanato)-ruthenium(II).⁶ The electrode was dipped into

* To whom correspondence should be addressed.

[®] Abstract published in *Advance ACS Abstracts*, March 1, 1997.

the dye solution while it was still hot, ca. 80 °C. As noticed by others,¹⁵ the uptake of the sensitizer was much slower for ZnO (days) compared to TiO₂ (hours).

Transmission and reflection measurements were performed on films supported on quartz substrates. The spectra were recorded using a Cary 2000 spectrophotometer equipped with an integrating sphere. Film thicknesses were determined using a Tencor Alpha Step profilometer. The surface morphology was studied by scanning electron microscopy (Jeol 25S II). The crystallite sizes for the ZnO (B) films were estimated from X-ray measurements using a Siemens D-5000 powder diffractometer. The resolution of the diffractometer was $0.15^\circ 2\theta$.

The experimental setup for the three-electrode measurements on the unsensitized films is described elsewhere.¹⁸ The transmission of the glass compared to air is used to compensate the absorption and reflection losses in the measurements. Since the transmission through the glass is less than 50% below 350 nm and the photocurrents are low, this part of the corrected back-side action spectra is uncertain. KI in water (0.1 M, purged with nitrogen, pH = 6.6) gave a high and stable photoresponse and was used as the electrolyte in the three-electrode experiments. The pH was adjusted by a 0.02 M potassium phosphate buffer. The applied potential at the working electrode was 0.3 V vs SCE where the highest photoconversion efficiencies were obtained.

In the two-electrode measurements (sandwich-type), the dye-sensitized ZnO electrode was squeezed together with a platinum foil using a spring. The electrolyte, 0.5 M LiI/0.05 M I₂ in ethylene carbonate/propylene carbonate (50:50% by weight), was attracted into the cavities of the ZnO electrode by capillary forces. No long-term stability tests were made. The incident photon-to-current conversion efficiency (IPCE⁶) for the dye-sensitized cells was measured with the two-electrode setup in short-circuit mode. To justify the experimental setup, we achieved similar photoconversion efficiencies for dye-sensitized TiO₂ as reported by Nazeeruddin et al.⁶ We obtained IPCE = 70% at 540 nm for a 6 μ m thick dye-sensitized TiO₂ film consisting of 15–20 nm large crystallites. The overall efficiency measurements were done with a 1000 W xenon lamp solar simulator (Spectral Energy Corp. LH 151N lamp housing, Spectral Energy Corp. LPS 255HR lamp power supply), together with a 1 cm water filter. The light intensity was measured by a pyranometer (Kipp & Zonen CM 11).

Results and Discussion

Figure 1a shows the SEM picture of a ZnO film prepared from powder A on conducting glass. The film consists of a three-dimensional network of interconnected particles having a size of approximately 150 nm. Roughly this is more than 1 order of magnitude larger than the size of the ZnO particles used in other investigations (cf. refs 13, 15, and 19). The particle size is also 1 order of magnitude larger than the size of the TiO₂ particles used in other studies.⁶ That particles shown in Figure 1a does not consist of even smaller particles is supported by X-ray diffraction. X-ray diffraction shows that the particles are significantly larger than 60 nm. A more accurate determination of the particle size with X-ray diffraction is not possible because of the experimental resolution. The SEM picture in Figure 1b shows the porous structure of a film prepared from powder B. From X-ray measurements by use of Scherrers formula, the crystallite size in ZnO (B) is estimated to be 15 nm (fwhm = $0.53^\circ 2\theta$ at the most intense peak).

In Figure 2 the incident photon-to-current conversion efficiency for front-side (illumination directly on the film) and back-side illumination (illumination through the supporting

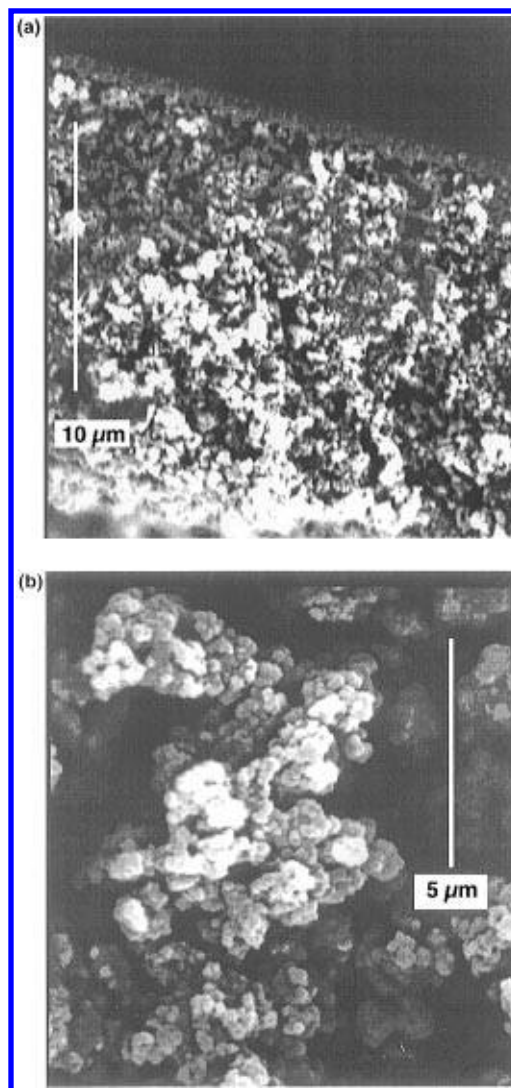


Figure 1. SEM picture of a nanostructured ZnO film deposited on a conducting glass for (a) films based on powder A and (b) films based on powder B.

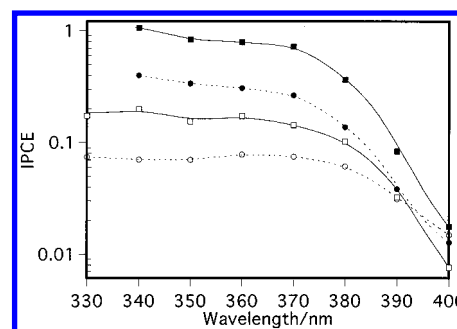


Figure 2. IPCE vs wavelength for 7 μ m thick ZnO (A) (solid line) and a 14 μ m thick ZnO (B) (dashed line) illuminated from different directions. For both films back-side illumination, i.e., through the conducting glass, gives higher efficiencies than front-side illumination. In the back-side illumination measurements, correction has been made for the reflection and absorption losses of the conducting glass. Since the transmission below 350 nm is low (below 50%), this correction is uncertain in the short wavelength region.

glass) for a 7 μ m thick ZnO (A) electrode is presented. The IPCE values follow the absorption spectra (Figure 3). The efficiency for back-side illumination of ZnO (A) film is higher than earlier reported results.^{13,19,20} Interestingly, we notice that at low wavelengths for front-side illumination, where the absorption and charge separation take place in the outermost layer of the film (see Figure 3), the nanostructured ZnO

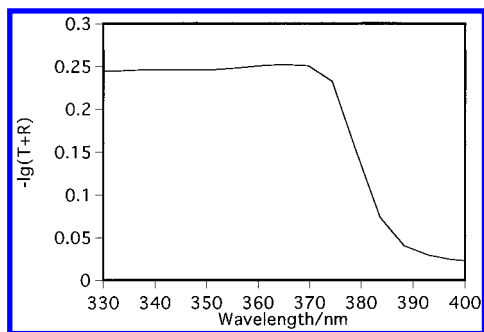


Figure 3. Spectra of $-\lg(T + R)$ for a less than $0.5 \mu\text{m}$ thick ZnO (A) film supported on quartz. $-\lg(T + R)$ is used instead of the absorption coefficient, since these films are highly light scattering and the $-\lg(T + R)$ is not necessarily proportional to the film thickness.

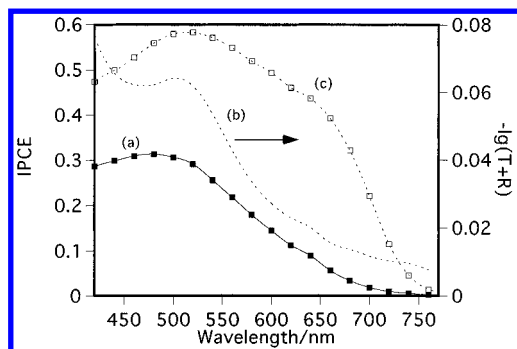


Figure 4. (a) IPCE vs wavelength for a dye-sensitized ZnO electrode (powder (A), film thickness of $9 \mu\text{m}$) measured using a two-electrode setup (left axis). (b) $-\lg(T + R)$ spectra for a less than $0.5 \mu\text{m}$ thick dye-sensitized electrode (right axis). (c) IPCE vs wavelength for a dye-sensitized ZnO electrode (powder (B), film thickness of $7 \mu\text{m}$) measured using a two-electrode setup (left axis).

electrodes still show good efficiencies. For ZnO (A), about one-fifth of the electrons are transported through the whole network, i.e., $7 \mu\text{m}$, without recombining. Also included in Figure 2 is the IPCE for front-side and back-side illumination of a $14 \mu\text{m}$ thick ZnO (B) film. High efficiencies are obtained, but in general they are lower than that of the ZnO (A) film. We can only speculate how the difference in particle size and Al content for ZnO (A) and ZnO (B) explains the difference in IPCE. For example the large Al-containing particles may reduce the resistance and/or give a lower probability for photocurrent losses. The conclusion from the results in Figure 2 is, however, that ZnO films have a good capability of transporting charges through the network and into the back-contact.

Two-electrode solar cell devices were produced using ZnO (A) and ZnO (B) films. Since the band gap and band edge position for ZnO and TiO_2 are similar, we used experimental conditions similar to the best reported for TiO_2 in this initial investigation,⁶ e.g., I^-/I_3^- as a redox couple. Figure 4a shows the IPCE spectrum in the visible region for a $9 \mu\text{m}$ thick dye-sensitized ZnO (A) electrode. The efficiency for the sensitized ZnO (A) has a maximum of about 30%. The films are highly light scattering, and a universal absorption coefficient applicable in a wide range of thicknesses for the dye-sensitized ZnO film is difficult to define. However, by measurement of the absorption in the visible region for a less than $0.5 \mu\text{m}$ thick dye-sensitized ZnO (A) electrode, it can be seen (Figure 4b) that poor light harvesting does not explain the lower efficiency in these ZnO (A) films compared to TiO_2 . Consequently, the reason for the lower efficiency must be explained by a lower injection efficiency or by an increase in photocurrent losses in dye-sensitized ZnO (A).

In Figure 4c we see that the IPCE for a $7 \mu\text{m}$ thick ZnO film prepared from powder (B) is higher. Maximum efficiencies of

50–60% was obtained at 540 nm. This is comparable with the results obtained for TiO_2 ,⁶ showing that ZnO-based electrodes can be considered as candidates for photoelectrochemical devices.

That the conversion efficiency for sensitized ZnO (B) is higher than sensitized ZnO (A) is interesting, since the results were opposite in the UV region for unsensitized films. This demonstrates differences in the charge separation process for an unsensitized and sensitized nanostructured film. The higher efficiency in our case, compared to Redmond et al.¹⁵ (IPCE at 520 nm = 13%, film thickness $0.8 \mu\text{m}$, crystallite size 10 nm), can mainly be attributed to a larger film thickness and thus a higher absorption in our electrodes.

Preliminary measurement for the overall energy conversion efficiency were also performed. For a $9 \mu\text{m}$ thick ZnO (A) film, illuminated with $30 \text{ mW}/\text{cm}^2$, the overall efficiency was 0.5% (short circuit current $1.1 \text{ mA}/\text{cm}^2$, open circuit voltage 0.37 V, fill factor 0.4, illumination area 1 cm^2). As indicated by the IPCE measurements (Figure 4), the efficiency is expected to be higher for the ZnO (B) films. Indeed, for a $30 \mu\text{m}$ thick ZnO (B) film an overall energy conversion efficiency of 2% at $56 \text{ mW}/\text{cm}^2$ light intensity was obtained (short circuit current $4.2 \text{ mA}/\text{cm}^2$, open circuit voltage 0.46 V, fill factor 0.6, illumination area 0.25 cm^2). It should be emphasized that when the cell is operated at high intensity, the counter electrode, surface treatment with coadsorbers, electrolyte concentration and viscosity, conducting glass resistance, etc., can be factors of importance for the overall efficiency. The effects of these factors have not been optimized in the present report.

In summary, we have fabricated dye-sensitized ZnO electrodes with high photoconversion efficiencies. Together with the earlier reported results,¹⁵ this investigation shows that a broad range of different particles is available for optimizing dye-sensitized nanostructured ZnO electrodes for photovoltaic applications. At the present stage, the monochromatic efficiency of dye-sensitized ZnO electrodes is only slightly less compared to that of dye-sensitized TiO_2 . However, the overall efficiency is still much lower. Thus, the challenge to reach the results reported on nanostructured TiO_2 systems remains.

Further work on ZnO is in progress, and we believe improvement can be accomplished by a thorough optimization of nanostructured ZnO systems with respect to, for example, dye, electrolyte composition, and coadsorbers. Moreover, to fundamentally understand how differences in nanostructured films, e.g., conductivity, affect the photoconversion efficiency, a more detailed investigation of different particle size, film thickness, and film morphology needs to be done.

Acknowledgment. This work was supported by the Swedish Materials Research Consortium on Clusters and Ultrafine Particles (which is funded by the Swedish National Board for Industrial and Technical Development (NUTEK) and the Swedish National Science Research Council (NFR)), the Swedish Research Council for Engineering Sciences (TFR), and the commission of the European Community Joule II program. We thank Professor Grätzel and co-workers for kindly supplying us with the dye and Nils-Olov Ersson for the help with the X-ray measurements. We also thank He Tianjing, Malin Abrahamsson, and Ted Larsson for their help in the development of the ZnO dispersions and Lionel Vayssieres for helpful discussions.

References and Notes

- (1) Gerischer, H.; Tributsch, H. *Ber. Bunsen-Ges. Phys. Chem.* **1968**, *72*, 437–445.
- (2) Gerischer, H.; Tributsch, H. *Ber. Bunsen-Ges. Phys. Chem.* **1969**, *73*, 850–854.

- (3) Tributsch, H.; Gerischer, H. *Ber. Bunsen-Ges. Phys. Chem.* **1969**, 73, 251–260.
- (4) Matsumura, M.; Matsudaira, S.; Tsubomura. *Ind. Eng. Chem. Prod. Res. Dev.* **1980**, 19, 415–421.
- (5) Hagfeldt, A.; Grätzel, M. *Chem. Rev.* **1995**, 95, 49–68.
- (6) Nazeeruddin, M. K.; Kay, A.; Rodicio, I.; Humphry, B. R.; Mueller, E.; Liska, P.; Vlachopoulos, N.; Grätzel, M. *J. Am. Chem. Soc.* **1993**, 115, 6382–6390.
- (7) O'Regan, B.; Grätzel, M. *Nature (London)* **1991**, 353, 737–740.
- (8) Hagfeldt, A.; Didriksson, B.; Palmqvist, T.; Lindström, H.; Södergren, S.; Rensmo, H.; Lindquist, S.-E. *Sol. Energy Mater. Sol. Cells* **1994**, 31, 481–488.
- (9) Knödler, R.; Sopka, J.; Harbach, F.; Grünling, H. W. *Sol. Energy Mater. Sol. Cells* **1993**, 30, 277–281.
- (10) Hagfeldt, A.; Björkstén, U.; Lindquist, S. E. *Sol. Energy Mater. Sol. Cells* **1992**, 27, 293–304.
- (11) Bedja, I.; Hotchandani, S.; Kamat, P. V. *J. Phys. Chem.* **1994**, 98, 4133–4140.
- (12) Björkstén, U.; Moser, J.; Grätzel, M. *Chem. Mater.* **1994**, 6, 858–863.
- (13) Hoyer, P.; Weller, H. *J. Phys. Chem.* **1995**, 99, 14096–14100.
- (14) Hodes, G.; Howell, I. D. J.; Peter, L. M. *J. Electrochem. Soc.* **1992**, 139, 3136–3140.
- (15) Redmond, G.; Fitzmaurice, D.; Grätzel, M. *Chem. Mater.* **1994**, 6, 686–691.
- (16) Wang, L.; Muhammed, M. *Synthesis of Controlled Morphology of ZnO Particles*, to be published.
- (17) Greenwood, N. N.; Earnshaw, A. *Chemistry of the elements*; Pergamon Press Ltd.: Oxford, 1984; pp 1403–1404.
- (18) Rensmo, H.; Lindström, H.; Södergren, S.; Willstedt, A.-K.; Solbrand, A.; Hagfeldt, A.; Lindquist, S.-E. *J. Electrochem. Soc.* **1996**, 143, 3173–3178.
- (19) Hotchandani, S.; Kamat, P. V. *J. Electrochem. Soc.* **1992**, 139, 1630–1634.
- (20) Björkstén, U. On the photoelectrochemistry of nanocrystalline porous metal oxide semiconducting electrodes. Nr. 1345; École Polytechnique Fédérale de Lusanne: Lusanne, Switzerland, 1995.